論文 / 著書情報
Article / Book Information

論題	
Title	Managing Both Strength and Ductility in Ultrafine Grained Steels
著者	辻 伸泰, 紙川直也, 上路林太郎, 高田尚記, 湖山裕文, 寺田大将
Author	Nobuhiro Tsuji, Naoya Kamikawa, Rintaro Ueji, Naoki Takata, Hirohumi Koyama, Daisuke Terada
掲載誌/書名	ISIJ International, Vol. 48, No. 8, pp. 1114-1121
Journal/Book name	ISIJ International, Vol. 48, No. 8, pp. 1114-1121
発行日 / Issue date	2008, 8
権利情報 / Copyright	本著作物の著作権は日本鉄鋼協会に帰属します。 Copyright (c) 2008 (THE IRON AND STEEL INSTITUTE OF JAPAN.

ISIJ International, Vol. 48 (2008), No. 8, pp. 1114–1121

Review

Managing Both Strength and Ductility in Ultrafine Grained Steels

Nobuhiro TSUJI,[1)] Naoya KAMIKAWA,[1,2)] Rintaro UEJI,[1,3)] Naoki TAKATA,[1,4)] Hirofumi KOYAMA[1)] and Daisuke TERADA[1)]

1) Dept. Adaptive Machine Systems, Graduate School of Engineering, Osaka University, 2-1 Yamadaoka, Suita 565-0871 Japan. 2) Materials Research Department, Risø National Laboratory for Sustainable Energy, Technical University of Denmark (Risø DTU), DK-4000, Roskilde, Denmark.
3) Faculty of Engineering, Kagawa University, 2217-20 Hayashi-cho, Takamatsu 761-0396 Japan.
4) Department of Metallurgy and Ceramics Science, Graduate School of Science and Engineering, Tokyo Institute of Technology, 2-12-1-S8-8, Ohokayama, Meguro, Tokyo 152-8552 Japan.

(*Received on April 14, 2008; accepted on May 8, 2008*)

Ultrafine grained (UFG) steels provide surprisingly high strength but sometimes show limited tensile ductility. In the present paper, systematic experimental results on mechanical properties of UFG steel with ferrite single phase are shown first. The limited tensile ductility of the UFG ferritic steel was due to very small uniform elongation, which was attributed to the early plastic instability in the UFG microstructures. This basic understanding suggested a way to overcome the low tensile ductility: if the strain-hardening of the matrix is enhanced by any means, both high strength and adequate ductility can be managed even in UFG structures. Actual examples of the UFG steels that could achieve good strength–ductility balance are also presented. Dispersing fine carbides within the UFG ferrite matrix, and making the UFG dual-phase structure composed of ferrite and martensite were both effective to manage high strength and large uniform elongation. It was clearly shown that the future studies on the UFG steels from practical viewpoint should be directed to make the UFG structures multi-phased.

KEY WORDS: strength; ductility; plastic instability; strain-hardening; multi-phase; dual phase; martensite.

1. Introduction

It has recently become possible at least on the laboratory scale to fabricate ultrafine grained (UFG) metallic materials with mean grain sizes smaller than 1–2 μm.[1–8)] In case of steels, there are two main ways to fabricate UFG structures: one is the thermomechanically controlled processing (TMCP) under hard conditions (such as very low finishing temperature and large reduction in one pass) using phase transformations,[3,4,7)] and the other is by severe plastic deformation (SPD) applying very high equivalent strain above 4–5.[4–6)] The obtained UFG steels show excellent mechanical properties, such as surprisingly high strength and good low-temperature toughness.[2–11)] However, the UFG steels have limited tensile elongation in many cases unfortunately.[9,10)] The aim of this review paper is firstly to make it clear why the tensile ductility is limited in the UFG materials. Based on this understanding, the second purpose is to show how we can overcome this issue, demonstrating several experimental examples of the UFG steels, in which both high strength and adequate ductility are managed, obtained in the authors' group.

2. Why Tensile Ductility Is Limited in UFG Steels

2.1. Experimental Evidence

Figure 1 shows engineering stress–strain curves of an ultralow-C interstitial free (IF) steel highly deformed by the accumulative roll bonding (ARB) process.[12,13)] The ARB is an SPD process using rolling deformation. The ARB principle and processing details have been shown in previous articles.[6,13–15)] The chemical composition of the IF steel used is shown in **Table 1**. The starting sheet had a fully recrystallized microstructure with a mean grain size of

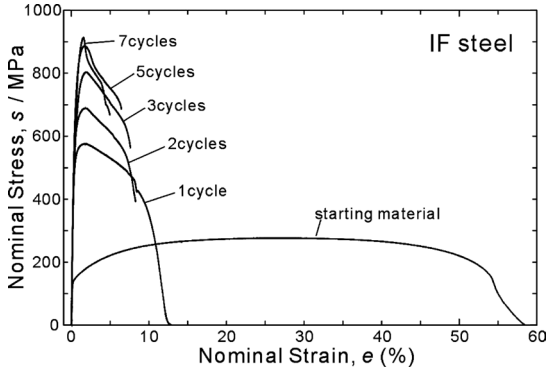

Fig. 1. Engineering stress–strain curves of the IF steel ARB processed by various cycles at 500°C without lubrication.

Table 1. Chemical composition of the IF steel studied (mass %).

C	N	Si	Mn	P	Cu	Ni	Ti	Fe
0.002	0.003	0.01	0.17	0.012	0.01	0.02	0.072	bal.

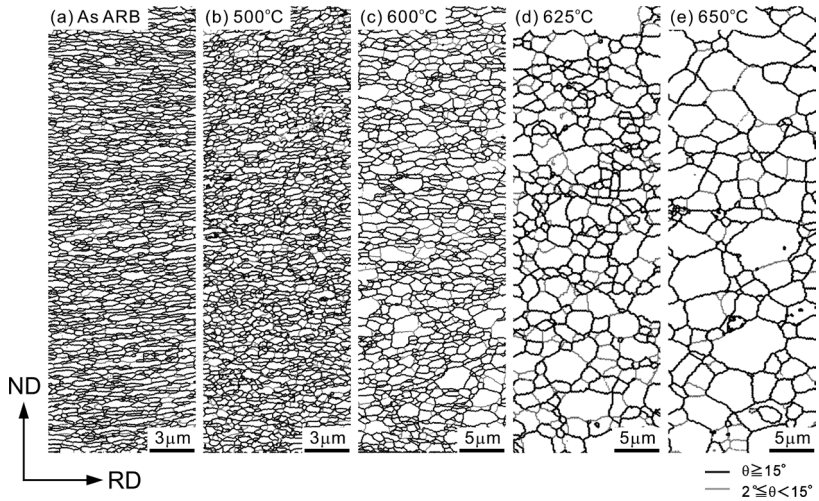

Fig. 2. Grain boundary map obtained by the EBSP analysis at thickness center of the IF steel ARB processed by 7 cycles at 500°C without lubrication and subsequently annealed at various temperatures for 1.8 ks. (a) as-ARB processed, (b) annealed at 500°C, (c) 600°C, (d) 625°C and (e) 650°C. Observed from TD.

20 μm. Two sheets of the IF steel with thickness of 1 mm were stacked, held at 500°C for 600 s in an electric furnace in an air Ar atmosphere, and then roll-bonded by 50% reduction in one pass without lubrication. These procedures correspond to the first ARB cycle. The roll-bonded sheet was cut into two, and the above mentioned procedures were repeated for the second ARB cycle. The ARB was repeated up to 7 cycles. Because equivalent strain of 50% rolling is 0.8, the total equivalent strain accumulated in 7 cycles of ARB is 5.6. Tensile specimens with gage width of 5 mm and gage length of 10 mm, which is 1 : 5 scaled version of JIS-5 standard tensile specimen, were cut from the sheets ARB processed by various cycles. Tensile test was carried out at room temperature (RT) at an initial strain rate of $8.3\times10^{-4}\,s^{-1}$. Tensile direction was parallel to the rolling direction (RD) of the sheets.

After only one ARB cycle (50% rolling), the strength of the IF steel greatly increased, as can be seen in Fig. 1. The tensile strength of the 1-cycle specimen was more than two times higher than that of the starting sheet. On the other hand, tensile ductility significantly decreased by the one ARB cycle. The stress–strain curve showed the maximum strength at early stage of tensile deformation, followed by macroscopic necking. Thus, the uniform elongation was limited within a few percent. This is a typical mechanical property of strain-hardened materials. With increasing ARB cycles (total strain), strength of the specimen monotonously increased and the tensile strength reached over 900 MPa after 7 cycles, which was 3.2 times higher than that of the starting material. Tensile ductility slightly decreased with increasing the applied strain. These are typical changes in mechanical properties of the SPD processed single phase materials.[8–10] It has been clarified in the parallel works that UFG structures with mean grain size of about 200 nm formed during the ARB process (after 5–7 ARB cycles).[10,12,16,17] It was, therefore, demonstrated that the UFG ferritic steel fabricated by SPD route certainly showed limited tensile ductility, especially limited uniform elongation. However, it has been also known that the UFG structures produced by SPD processes are, at the same time, deformation structures including high density of dislocations.[10,17,18] Thus, the limited ductility of the SPD materials may be attributed to the character of strain-hardened materials. Subsequently, the ARB processed IF steel sheets were annealed at various temperatures.[10,12,19]

The IF steel sheets ARB processed by 7 cycles at 500°C without lubrication were annealed at various temperatures ranging from 400 to 800°C for 1.8 ks. Orientation mapping by electron back-scattering pattern (EBSP) analysis was carried out for the ARB processed and annealed specimens on longitudinal sections perpendicular to the transverse direction (TD) of the sheets. A field-emission scanning electron microscope (FE-SEM; FEI Siron) equipped with a TSL-OIM system was operated at 20 kV for the EBSP measurement and analysis. **Figure 2** shows grain boundary maps of the ARB processed and annealed IF steel. In the maps, high-angle and low-angle boundaries are drawn in black and gray lines, respectively. The as-ARB processed specimen (Fig. 2 (a)) shows that the UFG structure is elongated parallel to RD. The mean thickness of the elongated grains was 210 nm. Transmission electron microscopy (TEM) images of the ARB processed and annealed IF steel are shown in **Fig. 3**. The TEM microstructures were observed from TD in a Hitachi H-800 operated at 200 kV. It was shown in Fig. 3(a) that the elongated UFGs contained many dislocations in the as-ARB processed state. By annealing at relatively low temperature, recovery in the grain interiors occurred decreasing the dislocation density within the UFGs (Figs. 3(b), 3(c)). After annealing at 600°C (Fig. 3(d)), almost all the grains were dislocation free, although the grain shape was still elongated slightly. At the same time, grain growth gradually happened with increasing annealing temperature, to make the grain size coarse (Figs. 2 and 3). The specimen annealed at 625°C (Figs. 2(d) and 3(e)) showed equiaxed grains free from dislocations, which cannot be distinguished from conventional recrystallized microstructures. However, the mean grain size of the 625°C annealed specimen was still very fine (1.6 μm), which cannot be obtained through conventional deformation and recrystallization. The change in the UFG structure (grain growth) was fairly uniform in this material, and typical (discontinuous) recrystallization characterized by nucle-

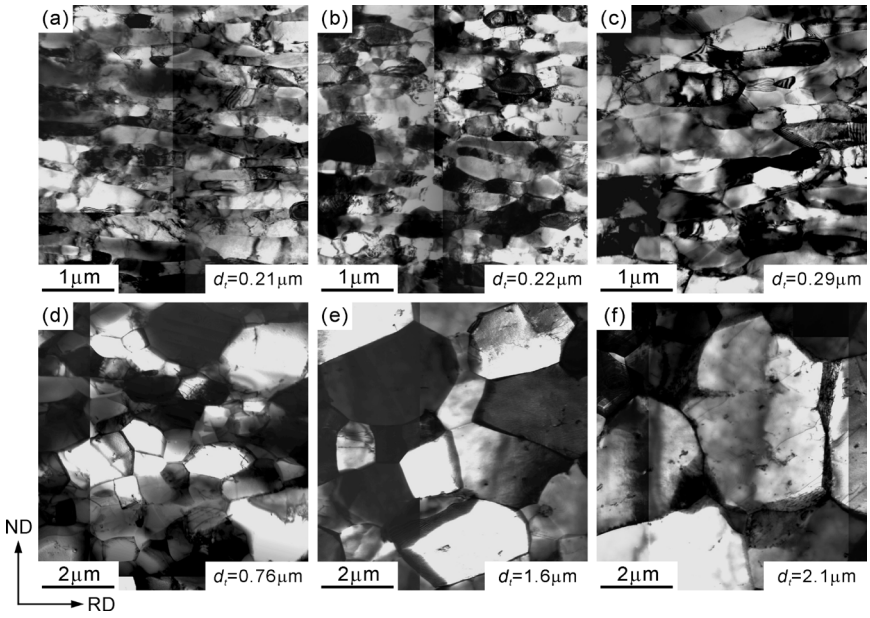

Fig. 3. TEM microstructures of the IF steel ARB processed by 7 cycles at 500°C without lubrication and subsequently annealed at various temperatures for 1.8 ks. (a) as-ARB processed, (b) annealed at 400°C, (c) 500°C, (d) 600°C, (e) 625°C, and (f) 650°C. Observed from TD.

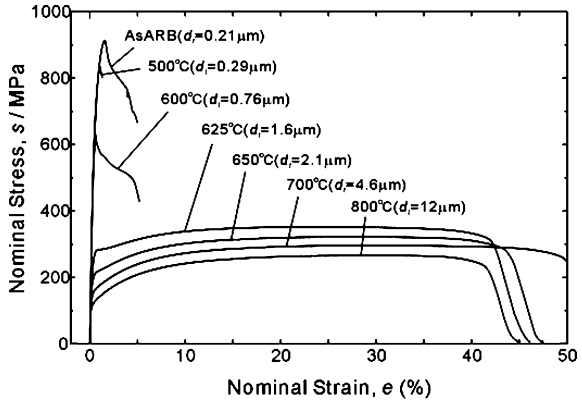

Fig. 4. Engineering stress–strain curves of the IF steel ARB proceseed by 7 cycles at RT without lubrication and then annealed at various temperatures for 1.8 ks. The annealing temperature and resulted mean grain size of each specimen are also indicated.

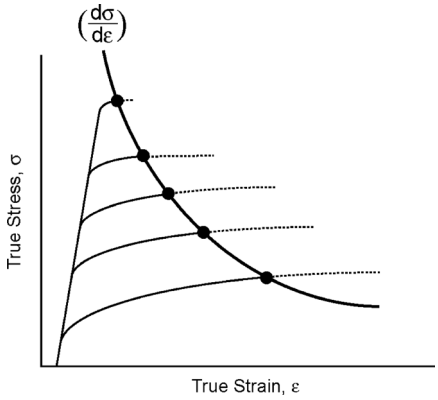

Fig. 5. Schematic illustration showing the change in plastic instability points as yield strength increases. It is assumed that the strain-hardening rate is constant.

ation and growth of particular grains was not recognized. Thus this process of microstructural change may be called "continuous recrystallization".[20)]

The engineering stress–strain curves of the ARB processed and annealed IF steel are shown in **Fig. 4**. The annealing temperature and resulting mean grain size of each specimen are also indicated in the figure. The strength of the specimens decreased with increasing annealing temperature (or with increasing mean grain size), while tensile ductility (uniform elongation) recovered only after the mean grain size became greater than 1 μm. As was mentioned above, the 600°C annealed specimen with a mean grain size of 0.76 μm had small number of dislocation within the grains. Thus, it can be concluded that the UFG ferritic steel having mean grain size smaller than 1 μm certainly shows limited tensile ductility, especially limited uniform elongation. Similar changes in mechanical properties have been found also in commercial purity Al and high purity (99.99%) Al with f.c.c. single phase matrix.[10,12)] Interestingly, the critical grain size above which the tensile ductility recovered was 1 μm in Al as well.

2.2. Reason for Limited Uniform Elongation

In the former section, it was confirmed that the UFG ferritic steel certainly showed limited tensile ductility, especially limited uniform elongation. Though only the experimental results for the ferritic IF steel were shown, a similar conclusion has been obtained also in austenitic steels[21)] and other metals like Al and Cu.[10,14,22)] The limited uniform elongation in the UFG metals can be understood in terms of plastic instability.[10,23)] Plastic instability corresponds to necking propagation during tensile testing, so that it determines the uniform elongation of the materials. The simplest equation for the plastic instability condition of strain-rate insensitive materials (typical metals) is known as,

$$\sigma \geq \left(\frac{d\sigma}{d\varepsilon} \right) \quad \text{.....(1)}$$

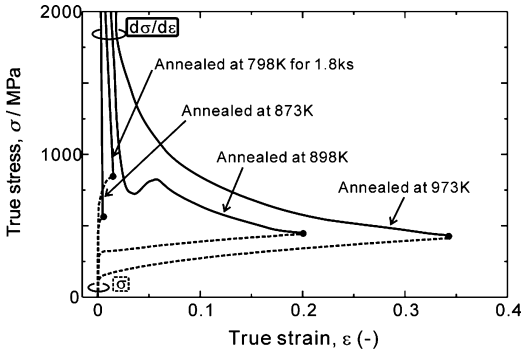

Fig. 6. True stress (broken lines) and strain-hardening rate (solid lines) as a function of true plastic strain in the IF steel ARB processed and then annealed at various temperatures for 1.8 ks. The positions at which two curves meet correspond to the plastic instability points.

where σ is flow stress (true stress) and $d\sigma/d\varepsilon$ is strain-hardening rate.[24] The condition can be schematically illustrated in **Fig. 5**. In the figure, yield strength of a material increases by any strengthening mechanisms such as grain refinement strengthening. Here it is assumed for simplicity that the strain-hardening rate does not change even if the material is strengthened. According to Eq. (1), the position at which two curves (flow stress (σ) and strain-hardening rate ($d\sigma/d\varepsilon$) meet is the plastic instability point. The figure clearly shows that the plastic instability condition is achieved at earlier stages of tensile deformation as the yield strength increases. Grain refinement raises the strength of metallic materials, and especially yield strength is significantly increased by fine grain structure. On the other hand, strain-hardening after macroscopic yielding is not enhanced by grain refinement, as can be seen from Fig. 4. Rather a decrease in strain-hardening has been found in the UFG Al.[10] Consequently, early plastic instability occurs in the UFG metals, resulting in limited uniform elongation in tensile tests.

The plastic instability condition was verified for the IF steel specimens ARB processed and annealed. **Figure 6** shows true stress (broken lines) and strain-hardening rate (solid lines) as a function of true plastic strain in the IF steel ARB processed and then annealed at various temperatures for 1.8 ks.[25] As was explained in Fig. 5, the points at which two curves meet correspond to the plastic instability condition. The strains at plastic instability points in Fig. 6 agreed well with the uniform elongation determined from the engineering stress–strain curves of the same specimens. This means that the uniform elongation of the UFG IF steel is certainly determined by plastic instability, as is discussed above.

3. How to Manage Both High Strength and Adequate Ductility in UFG Steels

In the previous section, it has been confirmed that the limited tensile ductility (limited uniform elongation) in the UFG ferritic steel is attributed to the early plastic instability. The early plastic instability seems an essential and inevitable feature of UFG microstructures. However, this understanding also tells us that the issue could be overcome if the strain-hardening rate of the UFG matrix is enhanced by any means. It should be noted that the UFG materials with limited tensile ductility reported in previous studies have been mostly single-phased materials like pure metals. By making the UFG structures multi-phased, for example, we may manage both high strength and adequate ductility even in UFG structures. Two experimental examples obtained in our group will be introduced in the following sections.

Table 2. Chemical composition of the SS400 steel studied (mass %).

C	N	Si	Mn	P	S	Fe
0.13	0.004	0.01	0.37	0.020	0.004	bal.

3.1. Dispersing Fine Carbides within UFG Ferrite Matrix

When we fabricate UFG structures in metals, large plastic strain is necessary in most cases of both TMCP and SPD routes. On the other hand, we have found that a type of UFG structure can be obtained without heavy deformation in low-C steels when as-quenched martensite is used as the starting microstructure.[25–29] When the as-quenched martensite is conventionally rolled by 30–70% reduction in thickness at RT and annealed at appropriate warm temperature, submicrometer UFGs can be formed. This easy fabrication of UFG structures is thought to be attributed to the characteristics of the microstructure of martensite in carbon steels.[27] Martensite in steels is a metastable phase having high free energy, and it is a type of fine-grain structure involving high density of lattice defects in the as-transformed state.[30] Additionally, it should be noted that the as-quenched martensite in steels is a supersaturated solid solution of carbon. Consequently, solute carbon precipitates as fine carbides within the ferrite matrix uniformly during warm-temperature annealing following conventional cold-rolling. That is, the obtained UFG structure through this route (martensite method) is a multi-phased UFG structure composed of UFG ferrite and finely dispersed carbides.[26,27]

A plain low-C steel (JIS SS400) having chemical composition shown in **Table 2** was used. Hot-rolled sheet 2 mm thick was austenitized at 1 000°C for 900 s and then water-quenched to obtain a martensitic structure. Since plain low-C steels have low hardenability, austenite grains were coarsened at a relatively high austenitizing temperature. The austenite grains coarsened to 270 μm in mean grain size, so that fully martensitic microstructure was obtained in the quenched specimen.[27] The as-quenched martensite was conventionally cold-rolled by 50% reduction in thickness in several passes. The cold-rolled specimen was annealed at various temperatures ranging from 400 to 600°C for 1.8 ks.

Figure 7(a) shows a TEM microstructure of the SS400 steel started from as-quenched martensite, cold-rolled by 50% and then annealed at 500°C for 1.8 ks. The microstructure was observed from TD. Nearly equiaxed UFGs with a mean grain size of 200 nm were observed. In this TEM observation, Kikuchi-line analysis of the identical area was carried out and misorientations between adjacent grains were calculated from the precise orientation data obtained. The result is represented as a boundary misorientation map in Fig. 7(b). The boundary misorientation map in-

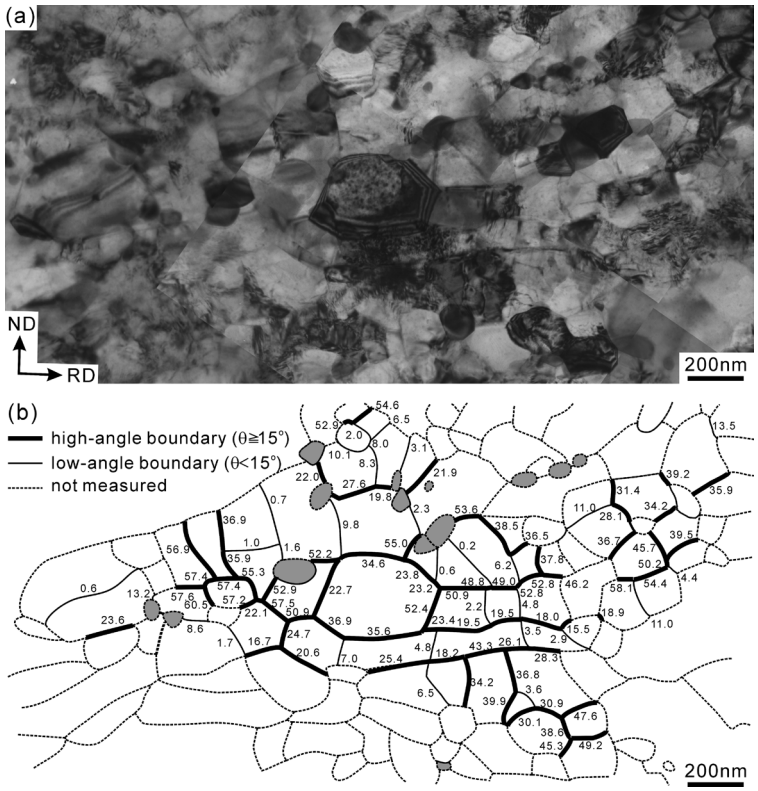

Fig. 7. TEM microstructure (a) and corresponding boundary misorientation map (b) of the SS400 steel started from as-quenched martensite, cold-rolled by 50% and then annealed at 500°C for 1.8 ks. Observed from TD.

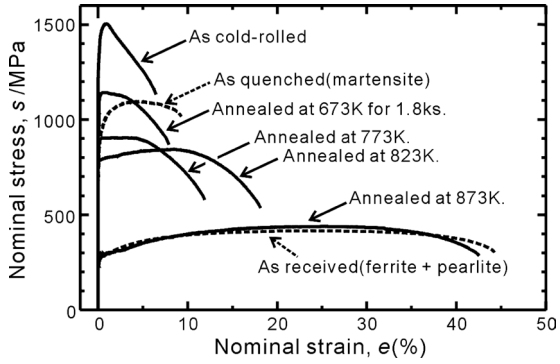

Fig. 8. Engineering stress–strain curves of the SS400 steel started from as-quenched martensite, cold-rolled by 50% and then annealed at various temperatures for 1.8 ks.

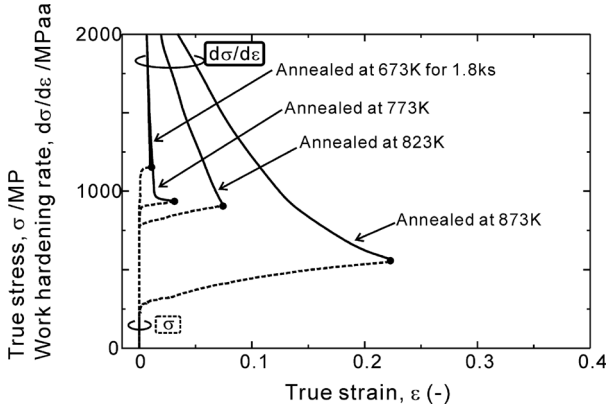

Fig. 9. True stress (broken lines) and strain-hardening rate (solid lines) as a function of true plastic strain in the SS400 steel started from as-quenched martensite, cold-rolled by 50% and then annealed at various temperatures for 1.8 ks. The positions at which two curves meet correspond to the plastic instability points.

dicated that many of UFGs are surrounded by high-angle boundaries. Within such ultrafine ferrite grains, a number of fine carbides (cementite) with various sizes precipitated uniformly. This is because the specimen before 500°C annealing was a supersaturated solid solution of carbon, as was described before. It is concluded, therefore, that the multi-phased UFG structure composed of ferrite and cementite is fabricated through the martensite method.

Engineering stress–strain curves of the SS400 steel specimens started from as-quenched martensite, cold-rolled by 50% and then annealed at various temperatures for 1.8 ks are shown in **Fig. 8**. Tensile tests were carried out under the same conditions described in Sec. 2.1. The as-rolled specimen showed very high strength over 1.5 GPa, but it had limited uniform elongation similar to the SPD material (Fig. 1). The flow stress decreased with increasing annealing temperature. However, the specimens annealed at 500°C or 550°C, that showed multiphased UFG structures of ferrite and cementite like Fig. 7, produced obvious strain-hardening after macroscopic yielding. As a result, these specimens illustrate adequate uniform elongation as well as high strength. Especially the 550°C (823 K) annealed specimen showed a 0.2% proof stress of 710 MPa, tensile strength of 870 MPa, uniform elongation of 8% and total elongation of 20%. Because the starting sheet was a 400 MPa class steel (JIS SS400), the multi-phased UFG specimen obtained had strength more than two times higher than that of the starting hot-rolled sheet with ferrite–pearlite structure.

In order to understand why the obtained specimen could

manage both high strength and adequate ductility, the plastic instability condition was again assessed for the specimens. The results are shown in **Fig. 9** in the same manners as Fig. 6. Strains at plastic instability points obtained in Fig. 9 corresponded well with the uniform elongation measured from the engineering stress–strain curves of the same specimens, which means that the uniform elongation of these specimens was again determined by plastic instability. Compared with Fig. 6 for the single-phased UFG steel, $(d\sigma/d\varepsilon)$ in Fig. 8 kept higher values after macroscopic yielding. This indicates that the finely dispersed carbides in the multi-phased UFG steel enhanced the strain-hardening to delay the plastic instability.[27] It is confirmed that dispersing fine precipitates (carbides) within the ferrite matrix is an effective way to manage both high strength and adequate ductility in UFG steels.

3.2. Ultrafine Grained Dual-phase Structure

In commercial steels for automobile applications, dual-phase (DP) structures composed of ferrite+martensite or ferrite+bainite are sometimes used for managing both high strength and ductility. If we can make UFG steels having DP structures, they are expected to show excellent mechanical properties. A low-C steel (JIS SM490; 490 MPa class) with chemical composition shown in **Table 3** was used for making UFG-DP structures. The hot-rolled sheets with ferrite+pearlite structure, though fraction of pearlite was very small in this low-C steel, were ARB processed by 6 cycles (equivalent strain of 4.8) at RT with lubrication. **Figure 10** shows a TEM image of the 6-cycle ARB processed specimen. Very fine lamellar structures of ferrite were elongated parallel to RD. The mean lamellar spacing was 60 nm. The lamellae sometimes showed a wavy morphology due to local shear banding. The as-ARB processed sample having such a microstructure was annealed at various temperatures between A_1 and A_3 (*i.e.*, in $\alpha+\gamma$ two phase region) for various periods. A high heating rate of 100 K s^{-1} was achieved by the use of induction heating system. After the intercritical annealing, the specimens were ice-brine quenched. **Figure 11** shows one of typical SEM microstructures of the ARB processed and intercritically annealed specimen. In the SEM image, ferrite and martensite reveal in dark and light contrasts, reapectively. During ice-brine quenching, the austenite (γ) transformed to martensite. The UFG-DP structure composed of UFG ferrite and UFG martensite was obtained. Both ferrite and martensite grains were nearly equiaxed. Each equiaxed martensite grain was probably transformed from identical austenite grain. Actually, a few packets were observed within each equiaxed martensite in EBSP analysis. The mean grain sizes of ferrite and martensite were 1.3 μm and 0.84 μm, respectively, and the fraction of martensite was 28.6% in this case. These microstructural parameters varied depending on the annealing conditions.

Engineering stress–strain curves of the SM490 steel

Table 3. Chemical composition of the SM490 steel studied (mass %).

C	N	Si	Mn	P	S	Nb	sol. Al	Fe
0.138	0.002	0.01	0.64	0.013	0.002	0.02	0.031	bal.

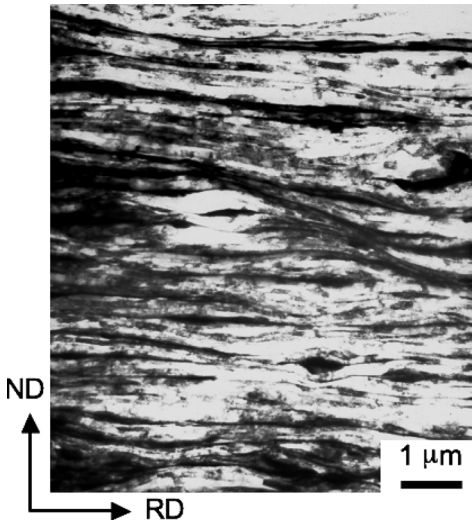

Fig. 10. TEM microstructure of the SM490 steel ARB processed by 6 cycles at RT with lubrication. Observed from TD.

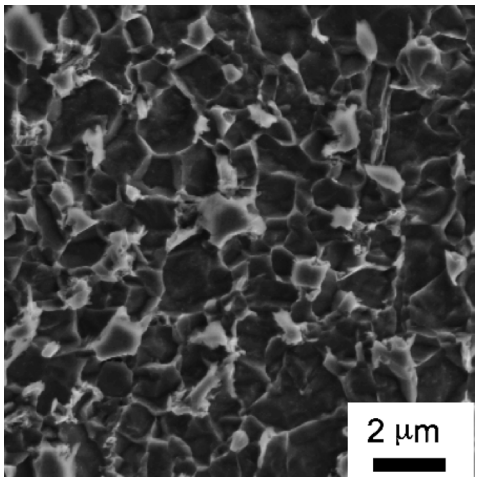

Fig. 11. SEM micrograph of the SM490 steel ARB processed by 6 cycles at RT with lubrication, intercritically annealed at 740°C for 60 s, and then ice-brine quenched. Observed from TD.

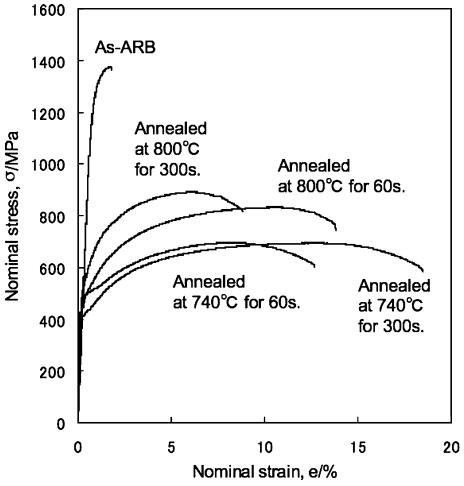

Fig. 12. Engineering stress–strain curves of the SM490 steel ARB processed by 6 cycles at RT with lubrication, intercritically annealed under various conditions, and then ice-brine quenched.

ARB processed, intercritically annealed and quenched are shown in **Fig. 12**. The as-ARB processed specimen performed very high strength of about 1.4 GPa but showed limited uniform and total elongation. Intercritical annealing greatly decreased the flow stress of the material, but all UFG-DP steels showed enhanced strain-hardening. As a result, fairly high strength and adequate tensile ductility were both managed in these specimens. It can be concluded, therefore, that dual-phase structures can provide a good strength–ductility balance even in UFG structures. Because the used steel had plain compositions, grain growth of nano-lamellae was not significantly suppressed even when a high heating rate was used. Addition of some kinds of alloying elements, such as strong carbide former (V, Ti, Nb, *etc.*), would inhibit grain growth during intercritical heat treatment to result in a much finer DP structure. Such nano-DP steels are expected to produce more excellent mechanical properties.

3.3. Concluding Remark

In the present paper, it was clearly shown that UFG steels with single phase certainly produce limited uniform elongation. The small uniform elongation is understood in terms of early plastic instability in the UFG microstructures. This understanding, however, also suggests a possibility to manage both high strength and adequate ductility in the UFG steels. Recently, Ma[31] pointed out several ways to get strength and ductility in UFG or nanocrystalline materials. His understanding also stands on the early plastic instability in such materials, so that most of the proposed ways aim to increase uniform elongation through enhancing strain-hardening, like the present study. The present work experimentally showed actual examples of UFG materials having both strength and ductility. However, they seem not the only ways to manage strength and ductility in UFG materials. For example, so-called TRIP (transformation induced plasticity) effect caused by deformation induced martensitic transformation might be applied to the UFG steels with certain chemical compositions.[31,32] Also it is a new and interesting finding that nanostructures with bimodal grain size distribution can show high strength and ductility.[23,33]

From a practical viewpoint, tensile ductility is certainly important. In this sense, the present work indicates that future studies on UFG steels should be directed to materials with "multi-phased" UFG structures. However, it should be also noted that the UFG metals show such instability only for tensile stress. Though tensile ductility is certainly limited, the UFG metals definitely do not lose plasticity and are not brittle. Actually, they show rather large post-uniform elongation in many cases, and it has been known that they can be heavily deformed in compression, rolling, bending, and so on. This should be emphasized even from a practical point of view.

Additionally, it has been recently found that the UFG metals sometimes show surprising properties that cannot be understood in terms of conventional metallurgy and materials science.[23,34–36] For example, the bimodal nanostructures that manage both strength and ductility[23,33] may provide a new idea of structure control. Furthermore, Huang *et al.*[35,36] have recently reported a "hardening by annealing and softening by deformation" phenomenon that is totally opposite to the conventional knowledge for metals and alloys. Such peculiar phenomena are due to the nanostructures where crystalline space is finly subdivided in nanometer scales by high-angle boundaries. These recent results suggest that further fundamental studies are desired for the UFG and nanostructured metals also from academic viewpoint, in order to pioneer a new frontier of metallic materials.

4. Summary

(1) Ultrafine grained (UFG) bulky steels of which mean grain size is smaller than 1–2 μm can be fabricated through various processing routes at least in laboratory scale. The UFG steels perform very high strength but have limited uniform elongation.

(2) It has been confirmed in the present paper that the limited uniform elongation of the UFG steels is attributed to early plastic instability caused by high yield strength and lack of strain-hardening capability in the UFG structures.

(3) The understanding of the reason for the limited ductility also indicates that the high strength and adequate ductility can be both managed if the strain-hardening of the UFG matrix is enhanced by any means.

(4) Actual examples of the UFG steels that could manage both high strength and adequate ductility were represented in the present work. The most important key is to make the UFG structures multi-phased.

Acknowledgements

This work was financially supported by the 14th steel research funding from ISIJ, grant-in-aid for scientific research on priority areas "giant straining process for advanced materials containing ultra-high density lattice defects" through the Ministry of Education, Sports, Culture, Science and Technology (MEXT) of Japan, and the industrial technology research grain program '05 through New Energy and Industrial Technology Development Organization (NEDO) of Japan (project ID 05A27502d). All these supports are deeply appreciated. The authors also thank Dr. Jake Bowen of Risø National Laboratory for his useful comments and English corrections on the manuscript.

REFERENCES

1) R. Z. Valiev, R. K. Islamgaliev and I. V. Alexandrov: *Prog. Mater. Sci.*, **45** (2000), 103.
2) S. Torizuka, K. Nagai and A. Sato: *J. Jpn. Soc. Technol. Plast.*, **45** (2001), 287.
3) Y. Hagiwara, M. Niikura, M. Shimotomai, Y. Abe and Y. Shirota: *J. Jpn. Soc. Technol. Plast.*, **45** (2001), 402.
4) N. Tsuji: *Tetsu-to-Hagané*, **88** (2002), 359.
5) Nanomaterials by Severe Plastic Deformation, ed. by M. J. Zehetbauer and R. Z. Valiev, Wiley-VCH, Weinheim, (2004).
6) Severe Plastic Deformation toward Bulk Production of Nanostructured Materials, ed. by B. S. Altan, NOVA Science Publishers, Inc., New York, (2006).
7) R. Song, D. Ponge, D. Raabe, J. G. Speer and D. K. Matlock: *Mater. Sci. Eng. A*, **A441** (2006), 1.
8) H. K. D. H. Bhadeshia: *Mater. Sci. Eng. A*, **A481–482** (2008), 36.
9) A. A. Howe: *Mater. Sci. Technol.*, **16** (2000), 1264.
10) N. Tsuji, Y. Ito, Y. Saito and Y. Minamino: *Scr. Mater.*, **47** (2002), 893.
11) N. Tsuji, S. Okuno, Y. Koizumi and Y. Minamino: *Mater. Trans.*, **45** (2004), 2272.

12) N. Kamikawa: PhD Thesis, Osaka University, (2006).
13) N. Tsuji: *J. Nanosci. Nanotechnol.*, **7** (2007), 3765.
14) Y. Saito, N. Tsuji, H. Utsunomiya, T. Sakai and R. G. Hong: *Scr. Mater.*, **39** (1998), 1221.
15) N. Tsuji, Y. Saito, S. H. Lee and Y. Minamino: *Adv. Eng. Mater.*, **5** (2003), 338.
16) N. Tsuji, R. Ueji and Y. Minamino: *Scr. Mater.*, **47** (2002), 69.
17) N. Kamikawa, T. Sakai and N. Tsuji: *Acta Mater.*, **55** (2007), 5873.
18) X. Huang, M. Tsuji, N. Hansen and Y. Minamino: *Mater. Sci. Eng. A*, **A340** (2003), 265.
19) N. Kamikawa, N. Tsuji and Y. Saito: *Tetsu-to-Hagané*, **89** (2003), 273.
20) F. J. Humphreys, P. B. Prangnell and R. Priestner: *Curr. Opin. Solid State Mater. Sci.*, **5** (2001), 15.
21) H. Kitahara, N. Tsuji and Y. Minamino: *Mater. Sci. Forum*, **503–504** (2006), 913.
22) N. Takata, S. H. Lee, C. Y. Lim, S. S. Kim and N. Tsuji: *J. Nanosci. Nanotechnol.*, **7** (2007), 3985.
23) Y. Wang, M. Chen, F. Zhou and E. Ma: *Nature* (*London*), **419** (2002), 912.
24) Fundamentals of Metal Forming, ed. by R. H. Wagoner and J. L. Chenot, John Wiley & Sons, Inc., New York, (1997).
25) R. Ueji: PhD Thesis, Osaka University, (2004).
26) N. Tsuji, R. Ueji, Y. Minamino and Y. Saito: *Scr. Mater.*, **46** (2002), 305.
27) R. Ueji, N. Tsuji, Y. Minamino and Y. Koizumi: *Acta Mater.*, **50** (2002), 4177.
28) R. Ueji, N. Tsuji, Y. Minamino and Y. Koizumi: *Sci. Technol. Adv. Mater.*, **5** (2004), 153.
29) N. Tsuji, R. Ueji and Y. Minamino: *Trans. Mater. Res. Soc. Jpn.*, **29** (2004), 3529.
30) H. Kitahara, R. Ueji, N. Tsuji and Y. Minamino: *Acta Mater.*, **54** (2006), 1279.
31) E. Ma: *JOM*, **58** (2006), 49.
32) T. Maekawa, H. Kitahara and N. Tsuji: *Adv. Mater. Res.*, **26–28** (2007), 413.
33) B. Srinivasarao, K. Oh-ishi, T. Ohkubo, T. Mukai and K. Hono: *Scr. Mater.*, **58** (2008), 759.
34) W. P. Tong, N. R. Tao, Z. B. Wang, J. Lu and K. Lu: *Science*, **299** (2003), 686.
35) X. Huang, N. Hansen and N. Tsuji: *Science*, **312** (2006), 249.
36) X. Huang, N. Kamikawa, N. Tsuji and N. Hansen: *ISIJ Int.*, **48** (2008), 1080.